



This discussion paper is/has been under review for the journal Natural Hazards and Earth System Sciences (NHESD). Please refer to the corresponding final paper in NHESD if available.

Empirical atmospheric thresholds for debris flows and flash floods in the Southern French Alps

T. Turkington¹, J. Ettema¹, C. J. van Westen¹, and K. Breinl²

¹University of Twente, Enschede, the Netherlands

²Paris-Lodron University of Salzburg, Salzburg, Austria

Received: 29 November 2013 – Accepted: 13 January 2014 – Published: 24 January 2014

Correspondence to: T. Turkington (t.a.r.turkington@utwente.nl)

Published by Copernicus Publications on behalf of the European Geosciences Union.

NHESD

2, 757–798, 2014

**Empirical
atmospheric
thresholds for flash
events**

T. Turkington et al.

Title Page

Abstract

Introduction

Conclusions

References

Tables

Figures



Back

Close

Full Screen / Esc

Printer-friendly Version

Interactive Discussion



Abstract

Debris flows and flash floods are often preceded by intense, convective rainfall. The establishment of reliable rainfall thresholds is an important component for quantitative hazard and risk assessment, and for the development of an early warning system. Traditional empirical thresholds based on peak intensity, duration and antecedent rainfall can be difficult to verify due to the localized character of the rainfall and the absence of weather radar or sufficiently dense rain gauge networks in mountainous regions. However, convective rainfall can be strongly linked to regional atmospheric patterns and profiles. There is potential to employ this in empirical threshold analysis.

This work develops a methodology to determine robust thresholds for flash floods and debris flows utilizing regional atmospheric conditions derived from ECMWF ERA-Interim reanalysis data, comparing the results with rain gauge derived thresholds. The method includes selecting the appropriate atmospheric indicators, categorizing the potential thresholds, determining and testing the thresholds. The method is tested in the Ubaye Valley in the southern French Alps, which is known to have localized convection triggered debris flows and flash floods. This paper shows that instability of the atmosphere and specific humidity at 850 hPa are the most important atmospheric indicators for debris flows and flash floods in the study area. Furthermore, this paper demonstrates that atmospheric reanalysis data is an important asset, and could replace rainfall measurements in empirical exceedence thresholds for debris flows and flash floods.

1 Introduction

A key component in risk assessments for natural hazards is quantifying the probability of occurrence in relation to specific intensities of the hazardous events. Intense short duration precipitation, long-lasting rainfall, and snowmelt are all potential triggers for hydro-meteorological hazards in mountainous areas in Europe (Brunetti et al., 2013;

NHESSD

2, 757–798, 2014

Empirical atmospheric thresholds for flash events

T. Turkington et al.

Title Page

Abstract

Introduction

Conclusions

References

Tables

Figures

⏪

⏩

◀

▶

Back

Close

Full Screen / Esc

Printer-friendly Version

Interactive Discussion



**Empirical
atmospheric
thresholds for flash
events**

T. Turkington et al.

Title Page	
Abstract	Introduction
Conclusions	References
Tables	Figures
⏪	⏩
◀	▶
Back	Close
Full Screen / Esc	
Printer-friendly Version	
Interactive Discussion	

Berti et al., 2012). Finally, many of the empirical methods establish a threshold above which debris flows may occur, without considering non-event observation also above the threshold, as there are many more non-event days. Meyer et al. (2012) used only debris flow events to determine the threshold, then analysed the annual frequency of days above the threshold. As rainfall is not the only factor governing debris flows, there will likely always be uncertainty in the definition of rainfall thresholds (Berti et al., 2012).

One way to approach the significance of a threshold is using Bayesian probability (e.g. Berti et al., 2012). Bayesian probability takes into account the likelihood of an event given certain conditions. However, while Bayes' theorem is useful in determining the probability of an event above a certain threshold, it does not take into account the probability that an event would be below this threshold. So even if the probability of an event occurring above a particular threshold is high, many events may occur below this threshold.

The thresholds above all use rainfall directly, however, it is also possible to analyse the cause of heavy precipitation. Ingredients that can lead to precipitation include mechanisms for uplift of an air mass (such as heating at the surface or orographic lift), increased saturation of the atmosphere, or a mixing of two or more air masses (such as fronts and low pressure systems). Maddox et al. (1979) found for the US that 43% of flash floods were caused by local convection, while the rest were synoptically driven. Studies in the Mediterranean basin show heavy precipitation events are often caused by quasi-stationary local convection (e.g. Nuissier et al., 2008). Atmospheric indicators can summarize the principle atmospheric conditions leading to heavy rainfall for a particular area, depending on the different causal mechanisms.

While atmospheric indicators have not had widespread usage in threshold analysis for flash events, they have been used as indicators for heavy rainfall and downscaling climate projections. Trapp et al. (2009) used the product of convective available potential energy (CAPE) and deep-layer wind shear (DLS) as an indicator for severe thunderstorms. Nuissier et al. (2011) used synoptic weather types based on the Hess–Brezowsky Grosswetterlagen classification, as well as low-level moisture flux and low-



**Empirical
atmospheric
thresholds for flash
events**

T. Turkington et al.

Title Page	
Abstract	Introduction
Conclusions	References
Tables	Figures
⏪	⏩
◀	▶
Back	Close
Full Screen / Esc	
Printer-friendly Version	
Interactive Discussion	

level wind direction to detect heavy precipitation events in southern France. Other examples of using atmospheric indicators for heavy precipitation include: Schmidli et al. (2007); Chen et al. (2010) and Jeong et al. (2012). Identification of synoptic (large-scale) atmospheric conditions that lead to flooding has also been undertaken in a number of studies (e.g. Petrow et al., 2009; Parajka et al., 2010).

Atmospheric indicators can be obtained using reanalysis data from physically-based models. Using a forecast model combined with observations, reanalysis data is both consistent with atmospheric observations and the laws of physics (Dee et al., 2011). The weighting given to the observations differs depending on the quality of the observations. Less reliable fields, such as precipitation, are less dependent on observations than more reliable fields such as mean sea level pressure (Tapiador et al., 2012). However, the quality of the output is dependent on the skill of the underlying forecasting model. Overall though, reanalysis data provides a wide range of atmospheric variables that are both spatially complete and coherent (Dee et al., 2011).

Rather than rainfall thresholds from local weather stations, this research develops empirical atmospheric thresholds for debris flows and flash floods using atmospheric indicators to identify the potential heavy rainfall events. The main advantages are that a dense observational rain gauge network is no longer required, and that there is no need to define explicitly what a rainfall event is. Furthermore, atmospheric thresholds can lead to a better understanding of the meteorological conditions that are related to the occurrence of debris flows and flash floods. Empirical atmospheric thresholds therefore can be an alternative to the conventional empirical rainfall thresholds where dense observational networks are not available, or where further investigation is required to the cause of the rainfall.

The structure of the paper is as follows: first an overview of the study area and the dataset is given, followed by a description of the methodology to develop atmospheric thresholds. The methodology includes dividing the flash events into those caused by local convection, and those that are from more synoptically driven, widespread rainfall. Thresholds using weather station data are also generated for comparison. The results



occurrence of larger events, although the events recorded depend on the exposure and awareness of the observers to the hazard (Ibsen and Brunsden, 1996; Carrara et al., 2003).

The historical inventory contains 29 flash floods and 39 debris flows events observed between 1979–2010, which occurred between March and November (Fig. 2). Tarolli et al. (2012) found a similar seasonal distribution of flash floods, with events generally occurring between August to November in the western Mediterranean. On average, discharge levels between September and November closely follows the mean precipitation intensity, while the discharge increases from March to July mainly due to snowmelt (Fig. 2). As the valley is orientated west-east, north facing slopes are likely to retain snow longer than south facing slopes.

Cepeda et al. (2010) developed Eq. (4) for debris flows based on hourly precipitation from Station 1. Only 7 debris flows were used, as the others occurred before sub-daily precipitation measurements were available (1998), or the precipitation or inventory record was deemed to be not sufficient (Cepeda et al., 2010). For the threshold, 86 % of the debris flow events used were correctly predicted, and 5.5 % of rainfall events above the threshold resulted in a debris flows. However, no threshold was obtained using only the longer daily rainfall dataset. To obtain a threshold for a longer time period, other methods or datasets are therefore required.

ECMWF ERA-Interim reanalysis data is used for analysing the regional atmospheric variables. The data has a spatial resolution of 80 km (T255) covering the period 1979–2012 (Dee et al., 2011). More information about observation and data assimilation and model characteristics for ERA-Interim can be found in Dee et al. (2011). The study area is approximately half of one grid box, so only the grid box containing the study area and those directly beside it are used (nine in total). The variables chosen (Table 2) contain commonly used predictors for statistical downscaling precipitation from Global Climate Models at multiple atmospheric pressure levels (Chen et al., 2010; Jeong et al., 2012). In addition, convective available potential energy (CAPE), deep layer shear (DLS), and soil moisture fields are also included. The first two are added as they might be in-

Empirical atmospheric thresholds for flash events

T. Turkington et al.

Title Page

Abstract

Introduction

Conclusions

References

Tables

Figures



Back

Close

Full Screen / Esc

Printer-friendly Version

Interactive Discussion



**Empirical
atmospheric
thresholds for flash
events**

T. Turkington et al.

Title Page	
Abstract	Introduction
Conclusions	References
Tables	Figures
⏪	⏩
◀	▶
Back	Close
Full Screen / Esc	
Printer-friendly Version	
Interactive Discussion	

Based on the availability of the weather station data and reanalysis data, the period 1979–2010 was chosen as the focus study period. The years from 1989 to 2004 are used for calibration and two validation periods are selected, namely 1979–1988 and 2005–2010. By splitting the validation period into two segments, changes in data quality, such as measurement techniques or observational coverage, are expected to be reduced while maintaining as long as possible data period. The probabilistic and static thresholds are also established using local weather station data for direct comparison with the empirical regional atmospheric thresholds.

3.1 Categorization of events

The proposed categories are based on the governing rainfall generation processes, with a secondary subdivision based on potential antecedent conditions. The four categories are: Ls – locally generated rainfall, spring, Lr – local rainfall, summer, Ss – synoptic (large scale atmosphere) rainfall, spring, and Sr synoptic rainfall summer. The classification is based on Merz and Blöschl (2008), who identify five categories for river floods based on the type of rainfall and antecedent conditions such as snowmelt and rainfall over several weeks. The categories Ls and Ss assume snowmelt is an antecedent condition, while Lr and Sr assume no snowmelt. For this study, seasonal antecedent conditions (snowmelt or/and rainfall) are based on the average annual discharge pattern in Sect. 2. From Fig. 2, the discharge generally returns to near baseflow levels in July. Added to this, the east-west orientation of the Ubye Valley means that the south facing slopes will be snow-free earlier than the north facing slopes. Therefore, the spring events were defined as flash events between March and June for south facing slopes, and between March to mid-July for north facing slopes.

The rainfall generation processes are split into types where local conditions are driving the generation, or whether it is governed by the synoptic atmospheric processes. In Done et al. (2006), the authors estimate the rate at which CAPE is being removed



by convective heating as:

$$t_{\text{CAPE}} \sim \frac{\text{CAPE}}{d\text{CAPE}/dt} \quad (6)$$

where t_{CAPE} is the convective timescale and $\frac{d\text{CAPE}}{dt}$ is the rate of change of CAPE removed by convective heating.

Done et al. (2006) suggest that with convective timescales shorter than 6 h the synoptic conditions are governing the instability of the atmosphere, while locally driven intense convection occurs when t_{CAPE} values are high. Non-convective precipitation would also have a low t_{CAPE} value, as CAPE values are generally low (Molini et al., 2011). Applying the criteria by Molini et al. (2011), flash events with $t_{\text{CAPE}} > 6 \text{ h}$ are classified as locally convective (L), and with $t_{\text{CAPE}} < 6 \text{ h}$ corresponding to more equilibrium conditions (S).

Molini et al. (2011) and Done et al. (2006) further modified Eq. (6) by estimating the latent heat release using the precipitation rate. However, as hourly rainfall rates are not available for any weather station before 1998, and Done et al. (2006) explain this is just a rough indication of the convective timescale, the version in Eq. (6) is used.

The accuracy of the classification of rainfall generation type is dependent on the accuracy of CAPE from ERA-Interim. Molini et al. (2011) found, when comparing CAPE values from ERA-Interim with those from a near-by radiosonde, there was only modest correlation, with a coefficient of determination of approximately 60%. Differences would be expected however, when comparing the grid box average with a point location.

3.2 Indicator selection

Each day in the calibration period 1989–2004 is assigned a label as an event day (a day where one or more flash events were recorded, and non-event days (where no flash event was recorded). The atmospheric indicators that show a distinction between event days and non-event days can then be used in the development of atmospheric

Empirical atmospheric thresholds for flash events

T. Turkington et al.

Title Page

Abstract

Introduction

Conclusions

References

Tables

Figures

⏪

⏩

◀

▶

Back

Close

Full Screen / Esc

Printer-friendly Version

Interactive Discussion



thresholds (Sect. 3.3). The silhouette index (SI) is used, as it takes into account both the separation between the clusters as well as the cohesion within the cluster (Rousseeuw, 1987). The index was developed as part of a tool to visualise the distinction between multiple clusters, and as a guide to the validity of the clustering and selection of number of clusters (Rousseeuw, 1987). It has since been used as a validation tool in classifying atmospheric conditions (e.g. Huth et al., 2008; Kannan and Ghosh, 2011; Kenawy et al., 2013).

An individual silhouette value determines how similar a point is to other points in its own cluster compared to points in other clusters (Rousseeuw, 1987). The SI then the average of all the silhouette values (Huth et al., 2008), with Eq. (7) valid for two clusters:

$$SI = \frac{1}{2} \sum_{c=1}^2 \frac{1}{n_c} \sum_{i=1}^{n_c} \frac{b_i - a_i}{\max(a_i, b_i)} \quad (7)$$

where n_c is the number of observations in cluster c , b_i is the average Euclidean distance between an observation i and all observations in the other cluster and a_i is the average Euclidean distance between i and all observations in the same cluster.

The SI varies between -1 and 1 . An individual silhouette value of 1 indicates that the observation is correctly classified, while a near zero value indicates that the observation could belong to either cluster, and negative values indicate misclassification (Ansari et al., 2011). The highest SI indicates the best clustering (Ansari et al., 2011). An SI value of 1 means that the clusters are compact and well separated from each other (Kenawy et al., 2013).

A worked example of the SI for floods in the Ubaye River is given. Days with high discharge values (flood days) are compared with no-flood days. The no-flood days chosen had similar event and antecedent rainfall amounts as the flood days. Figure 3 shows the individual silhouette values for flood days/and no-flood days in the Ubaye Valley based on $Q850$ and U and $V850$. The left figure shows the individual silhouette values for each flood day are above 0 , indicating they are more similar to the other

Empirical atmospheric thresholds for flash events

T. Turkington et al.

Title Page

Abstract

Introduction

Conclusions

References

Tables

Figures

⏪

⏩

◀

▶

Back

Close

Full Screen / Esc

Printer-friendly Version

Interactive Discussion



Empirical atmospheric thresholds for flash events

T. Turkington et al.

Title Page

Abstract

Introduction

Conclusions

References

Tables

Figures

⏪

⏩

◀

▶

Back

Close

Full Screen / Esc

Printer-friendly Version

Interactive Discussion

flood days that the no-flood days. For the no-flood days, half of the days have positive silhouette values and are likely correctly classified. The other half have negative values, indicating they are more similar to the flood days. The figure on the right side plots the no-flood and flood days, and shows the separation between the two groups. It shows that generally flood days have higher specific humidity and more easterly winds compared with no-flood days.

The SI value is less reliable for clusters when there is a large difference between the observations in each of the clusters. Therefore, x days are randomly selected to calculate the SI using the normalized atmospheric variables, where x is the number of flash events. This is repeated multiple times (10 000), with variables with the highest mean SI value selected for threshold analysis. Any atmospheric indicators that had more than 10 % of SI values less than zero were discarded. In Sect. 4.2, only the mean SI value is given.

As conventional thresholds are generally defined using two variables, the analysis is performed with the two best performing indicators. Furthermore, too many indicators could create noise, or lead to over-fitting of the data.

3.3 Probabilistic and static thresholds

Bayes' theorem expresses the conditional probability of an event A occurring given some condition or conditions, B (Eq. 8). It is based on the unconditional probability of A occurring, $P(A)$, unconditional probability of the condition occurring $P(B)$, and the conditional probability of $P(B|A)$.

$$P(A|B) = \frac{P(B|A)P(A)}{P(B)} \quad (8)$$

Using the two indicators from Sect. 3.2 that had the highest SI value, the probability of a flash event occurring was calculated over the observed range of each of the indicator. This is similar to Berti et al. (2012), although extended to using atmospheric indicators.

**Empirical
atmospheric
thresholds for flash
events**

T. Turkington et al.

Title Page	
Abstract	Introduction
Conclusions	References
Tables	Figures
◀	▶
◀	▶
Back	Close
Full Screen / Esc	
Printer-friendly Version	
Interactive Discussion	

A limitation of using probability of occurrence is that it does not take into account the percentage of flash events above the threshold. Therefore, a static threshold is also determined considering both the number of events above and below the threshold. A static threshold is taken to be a threshold where the values of the indicators remain constant. The indicators used for the static threshold are the same as for the probabilistic threshold.

A confusion matrix displays the performance of a prediction algorithm, such as a static threshold. The four classifiers in the confusion matrix (Mason and Graham, 1999) are:

- True positives (TP): the number of correctly predicted events
- False positives (FP): the number of events predicted, but where no event occurred
- False negatives (FN): the number of events that were not predicted
- True negatives (TN): the number of days that were correctly predicted as non-events

These classifiers can then be used to determine the correlation between the predicted and observed results using the Matthews Correlation Coefficient (MCC; Powers, 2011):

$$MCC = \frac{TP \times TN - FP \times FN}{\sqrt{(TP + FP) \times (TP + FN) \times (TN + FP) \times (TN + FN)}} \quad (9)$$

The MCC is similar to the Pearson’s product–moment correlation coefficient applied to contingency tables (Powers, 2011). A value of 1 indicates perfect correlation, while zero indicates no relationship and negative values indicate negative correlation. Although to our knowledge the MCC has not been used in rainfall threshold assessment, it has been used in bioinformatics, as an assessment tool where there are unequal events and non-events (Baldi et al., 2000; D’Este and Rahman, 2013).



The MCC is calculated for each combination of atmospheric indicators from the probabilistic threshold. The threshold with the highest MCC value is chosen as the static threshold, with the added condition in that at least 50% of the flash events are also above the threshold. These selection criteria are somewhat subjective, as the optimal threshold will depend on the application.

4 Results and discussion

4.1 Categorization of events

Table 3 shows the t_{CAPE} value (Eq. 6) for all separate events in the period 1989–2004. In 66% of the events, local convection was considered to be the dominant meteorological trigger for flash events in the Ubaye Valley. The earliest local convective event reported in a year occurred on the 1 June and the latest on the 23 November (number 13 in Table 3). The synoptic events occurred over a wider range of months, between March (number 9) and November (number 1).

It is possible that some of the flash events are in the wrong category. Four of the nine synoptic events had no rainfall recorded in at least half of the stations 1–4, which would not be expected with widespread rainfall (numbers 3, 4, 6, 8 in Table 3). However, any misclassification would likely only reduce the efficiency of the clustering (Sect. 4.2), and the significance of the thresholds (Sect. 4.3). Therefore we used the classification as indicated in Table 3 for the subsequent analysis.

4.2 Indicator selection

The two best performing indicators for the local convective events were CAPE and specific humidity at 700 hPa (Fig. 4). These indicators showed the highest SI value, 0.32 (apart from using only Q_{700}). CAPE especially has been used before as an indicator for intense convection (Marsh et al., 2009), as it indicates atmospheric instability. Q_{850}

Empirical atmospheric thresholds for flash events

T. Turkington et al.

Title Page

Abstract

Introduction

Conclusions

References

Tables

Figures



Back

Close

Full Screen / Esc

Printer-friendly Version

Interactive Discussion



is indicative of low-level moisture, which is also necessary for locally generated precipitation. Comparatively, the U and V winds showed very low SI values, indicating that wind conditions do not separate flash event days from non-event days. This was also true for DLS and soil moisture (SWL). Temperature, vorticity and divergence showed moderate SI values, between 0.1 and 0.25 depending on what other atmospheric indicator it was paired with. The moderate SI values separate the flash events from the non-event days somewhat, but not as much as CAPE and Q850.

Figure 5 (top) shows that for all the synoptic events, only 10 indicator combinations were significant (at $p = 0.10$). The highest SI value (0.15) was also half of the value found for local convective events. As the number of significant indicator pairs was low, the SI was calculated again further splitting the events into the Ss and Sr categories (Fig. 5 middle and bottom). However, this was a trade-off between the limited number of events belonging to each classification and potential differences in indicators.

Splitting the synoptic events into the Sr and Ss categories showed differences between the atmospheric indicators with the highest SI (Fig. 5). For Ss events, temperature at multiple pressure levels separated days with flash events from days with no flash events. This was in combination with 8 day average mid-level divergence, temperature, CAPE or specific humidity. The highest SI value of 0.21 was for temperature (3 day) and specific humidity (8 day), both at 700 hPa. These two indicators were then used as the basis of the thresholds in Sect. 4.3. For the Sr flash events, the significant indicators were divergence at 700 hPa (daily), low level specific humidity, SWL, and 8 day average temperature (Fig. 5). The highest SI of 0.42 for the Sr flash events corresponded to specific humidity and 8 day average temperature at 700 hPa. Low level moisture ($Q700$ and $Q850$) again appeared to be a key atmospheric indicator. Low level temperature was also a key indicator, although only when Ss and Sr events were separated (Fig. 5). It was possible that one class was associated with colder temperatures, and the other with warmer temperature, which then cancel when combined.

Finally, for the local weather station data, the highest SI value of 0.29 was for the 4 day and daily total rainfall based on the data from station 3. Other stations and combi-

Empirical atmospheric thresholds for flash events

T. Turkington et al.

Title Page

Abstract

Introduction

Conclusions

References

Tables

Figures

⏪

⏩

◀

▶

Back

Close

Full Screen / Esc

Printer-friendly Version

Interactive Discussion



nation of stations were tried, but had lower SI values. These indicators were similar to those for debris flows in Jaiswal and van Westen (2009), where 1 and 5 day totals were used. A four-day antecedent period was chosen over five-day as it had a slightly higher SI value (0.29 compared with 0.27). Intensity and duration indicators are not used, as hourly data were not available before 1998. Also, previous attempts using daily data showed all flash events were below the thresholds Eqs. (2) and (3).

4.3 Probabilistic and static threshold

4.3.1 Weather station thresholds

Using the daily values and four-day values for antecedent conditions, a threshold was generated that showed increasing chance of flash events with higher rainfall totals. The highest probability of a flash event was 17% when the one-day total is above 80 mm and the four-day above 96 mm (Fig. 6). This is lower than the maximum probability found in the study by Berti et al. (2012) of 40–60%.

While Fig. 6 seems reasonable (more precipitation, more likely for a flash event to occur), there are a few limitations. There are nine days with precipitation totals above 82 mm where no flash event was recorded and hence zero probability of flash occurrence. The lack of recorded events may have been because of low precipitation intensity, or the amount recorded by the rain gauge was much higher than for the rest of the study area. Spatial heterogeneity of rainfall may also be the reason why during the calibration period no precipitation was recorded for one flash event, and less than 10 mm for a further six flash events.

For the static threshold, the maximum MCC value during the calibration period, with at least 50% of events above the threshold, corresponded to the following Weather Station threshold (Thres_{WS}):

- Thres_{WS} : one-day precipitation > 20 mm and four-day antecedent precipitation > 22 mm.

Empirical atmospheric thresholds for flash events

T. Turkington et al.

Title Page

Abstract

Introduction

Conclusions

References

Tables

Figures

⏪

⏩

◀

▶

Back

Close

Full Screen / Esc

Printer-friendly Version

Interactive Discussion



**Empirical
atmospheric
thresholds for flash
events**

T. Turkington et al.

Title Page	
Abstract	Introduction
Conclusions	References
Tables	Figures
⏪	⏩
◀	▶
Back	Close
Full Screen / Esc	
Printer-friendly Version	
Interactive Discussion	

The values for the static threshold are given in Table 4. Only 8.5 % of the total number of days were above the $\text{Thres}_{\text{WS}}((\text{TP} + \text{FP})/(\text{FN} + \text{TN}))$, while 55 % of the flash events were above the $\text{Thres}_{\text{WS}}(\text{TP}/(\text{TP} + \text{FN}))$. Somewhat surprisingly, 45 % of the event days had less than 20 mm of rainfall. The percentage of the total number of days above Thres_{WS} was slightly lower for the two validation periods (7.5 % and 6.1 % respectively), and the percentage of flash events drops even more (35.7 % and 33.3 % respectively).

While the likelihood of a flash event still remains higher for days above the static threshold in the validation period, the drop in percentage of flash events above the threshold indicates differences in the triggering conditions between the calibration and validation periods. As both the validation periods are different, this suggests that the changes are not completely from changes in the landscape or mitigation works. The torrents in which flash events occurred are generally closer to station 3 in the earlier validation period than the calibration period.

The results for the static threshold are comparable to those from other studies. Cepeda et al. (2010) found for the same study area that their threshold is exceeded on average 8.6 times per year, while 60 % of debris flows are above the threshold (if including all debris flows between 1998 and 2010). While the percentage of correctly predicted events is slightly lower, the percentage of false positives is only a third of the amount using Eq. (4). The better performance of the rainfall threshold using hourly data from Station 1 indicates that rainfall intensity is important rather than daily amount. The daily total of 20 mm was in the range of Meyer et al. (2012), between 15–107 mm day⁻¹. The probability of static threshold exceedence was also similar to Meyer et al. (2012), whose threshold was exceeded between 0 and 77 days in a year (8.5 % corresponds to 31 days a year).

4.3.2 Atmospheric thresholds: local convection

Flash events during the summer and autumn period are more likely under high instability (CAPE) and high 700 hPa specific humidity (Fig. 7). As both the instability of the atmosphere and low level moisture increase in Fig. 7, the probability of a flash event



also increases. High instability but low moisture (so less probable raincloud development) show low probability of a flash event, as is expected. The highest probability (100 %) is higher than found in Sect. 4.3.1 and from Berti et al. (2012). This corresponds to CAPE values above 1100 Jkg^{-1} and normalized $Q700$ greater than 1.45, although this has only been observed once between 1989 and 2003.

For the static threshold, the maximum MCC value during the calibration period, corresponded to the following threshold (Thres_L):

– Thres_L : CAPE $> 250 \text{ Jkg}^{-1}$ and normalized specific humidity at 700 hPa > 0.40 .

The confusion matrix results and MCC values are shown in Table 4. From this table it can be seen that 6.8 % of the days are above Thres_L , compared with 75 % of local convective flash events. In the validation periods, the percentage of days above Thres_L rises to 7.8 % (Validation Period 1) and 7.3 % (VP2) and 71 % and 80 % for the local convection flash events.

Compared with the results in Sect. 4.3.1, both the probability threshold and static thresholds perform better for the local convection than for the weather station threshold. Figure 7 shows higher probabilities of flash event occurrence than Fig. 6. Similarly, the MCC value for all three periods was higher for the local convection atmospheric threshold. And in both validation periods, more flash events were above the Thres_L than Thres_{WS} , with an even smaller number of FPs in the first validation period. Lower number of FP is important for early waning systems where the number of false alarms should be minimised.

While the CAPE value in Thres_L was low for intense convection, similar limits have been found in other studies (e.g. for hail Niall and Walsh, 2005; Pistotnik et al., 2011, for heavy rainfall). Trapp et al. (2009) also found that availability of low level water vapour was a key component of changes in severe convection at mid-latitudes.

Empirical atmospheric thresholds for flash events

T. Turkington et al.

Title Page

Abstract

Introduction

Conclusions

References

Tables

Figures

⏪

⏩

◀

▶

Back

Close

Full Screen / Esc

Printer-friendly Version

Interactive Discussion



4.3.3 Atmospheric thresholds: synoptic, spring

Based on Sect. 4.2, it appears when the Ss and Sr events are grouped together that the resulting SI values are low, performing better than when the SI values are calculated individually (Fig. 5). However this meant that there were only 4 to 5 flash events in each group, only two or three more than the number of indicators. Therefore, the thresholds were unlikely to be as robust as for the local convection and weather stations, as there were fewer events to both calibrate and validate the thresholds.

Figure 8 shows for Ss indicators, that with warmer 700 hPa temperatures and higher specific humidity the probability of flash event occurrence increases. Warm low to mid-level temperatures could be associated with melting of snow and high moisture levels could indicate rain. Figure 8 had similar probabilities of occurrence compared to Thres_{WS} , with the highest probability of occurrence of 12.5%. Similar to Fig. 6, the most extreme days (days with the highest 8 day moisture and warmest 3 day temperature), were not associated with flash events.

Using the criteria in Sect. 3.3 resulted in the following threshold (Thres_{SS}):

- Thres_{SS} : three-day mean temperature at 700 hPa > 271 K and eight-day mean normalized specific humidity at 700 hPa > 0.70.

The values for the confusion matrix and MCC are in Table 4. Only 4.3 % of days are above Thres_{SS} , and 50 % of the flash events. In the validation periods, the percentage of days above the threshold increased to 7.4 % (Validation period 1) and 7.2 % (VP 2), while only one of the three days in the first validation period was above the threshold. In the second validation period, there were no events in this category.

As was in Thres_{SS} , if the three-day average temperature at 700 hPa (lower troposphere) is be above 271 K, then the majority of the study area would be at above freezing temperatures. While snow could still fall at the highest elevations, it is likely that it would rain in lower regions, and that any snow on the ground may melt. The second requirement of Thres_{SS} , specific humidity at 700 hPa being higher than normal, also

Empirical atmospheric thresholds for flash events

T. Turkington et al.

Title Page

Abstract

Introduction

Conclusions

References

Tables

Figures



Back

Close

Full Screen / Esc

Printer-friendly Version

Interactive Discussion



while the threshold was reasonable during the calibration period, it did not hold for the validation periods.

Colder temperatures during a summer synoptic flash event are not unreasonable. Lower temperatures in summer may be associated with a front passing or cooler temperatures from prolonged cloud cover (and potentially rainfall). Similar to the other three atmospheric categories, high specific humidity indicated higher atmospheric moisture and more likely rain. However, Thres_{Sr} was unsuccessful in the validation period. It could be that different synoptic conditions lead to flash events in the two validation periods, or that the events were misclassified.

4.3.5 General discussion

As with any empirical threshold, accuracy and completeness of the inventory and weather data are important. During the classification and subsequent threshold analysis, it is possible that flash events were misclassified. The resolution of ERA-Interim was not fine enough to explicitly resolve convection, hence parameterization schemes are used, although Dee et al. (2011) show improvements in the convection parameterization from earlier reanalysis products. Furthermore, as the CAPE values take into account instability over the depth of the troposphere, CAPE values may be underestimated when convection is confined to a shallow layer (Niall and Walsh, 2005). As found in Sect. 4.1, it is likely that some events may have been misclassified as local convection or as synoptic.

As synoptic flash events generally performed the worst, further investigation on these nine events was undertaken. Based on the Hess–Brezowsky Grosswetterlagen synoptic weather type (James, 2007), all synoptic flash event days except the 19 August 1996 event show evidence of a low pressure system near the study area. With the small number of events and variety of different locations of the fronts or low pressures, it may not have been possible to use the traditional threshold-type approach for these events. A potential solution could be to identify key groups of indicators instead. Therefore, further investigation would be needed to determine if (a) the events were correctly

Empirical atmospheric thresholds for flash events

T. Turkington et al.

Title Page

Abstract

Introduction

Conclusions

References

Tables

Figures



Back

Close

Full Screen / Esc

Printer-friendly Version

Interactive Discussion



dated, (b) caused by synoptic meteorological triggering conditions or (c) triggered by non-meteorological factors.

Atmospheric thresholds, like most empirical thresholds, are reliant on near-complete inventories, and only speculations can be made about what may happen under unobserved conditions. Therefore, these methods cannot completely replace physically based models and other threshold analysis techniques. However, for the Ubaye Valley where local convection appears to be the main meteorological trigger of flash events, the atmospheric threshold improves on the local rainfall threshold. This methodology therefore has a potential to work in other areas where rainfall observations are not available, or not complete enough for the traditional empirical rainfall threshold.

5 Summary and conclusions

The objective of this research was to develop empirical thresholds for rainfall triggered debris flows and flash floods using atmospheric indicators. Similar to rainfall thresholds, these thresholds could be used in risk assessment, early warning systems, or climate change projections. Empirical atmospheric thresholds were obtained for the Ubaye Valley, France, as well as weather station derived rainfall thresholds for comparison. In each case two types of thresholds were obtained: a probability threshold and a static threshold, based on classification statistics and specifically the MCC value. The main conclusions are as follows:

- In general the atmospheric indicators performed better than the weather station threshold (average MCC value of 0.16 compare with 0.10, and higher probability of occurrence). They also performed better than rainfall thresholds using hourly data.
- The most important atmospheric indicators were CAPE and specific humidity at 850 hPa. Both fit with convective precipitation being the main driver.

Empirical atmospheric thresholds for flash events

T. Turkington et al.

Title Page

Abstract

Introduction

Conclusions

References

Tables

Figures



Back

Close

Full Screen / Esc

Printer-friendly Version

Interactive Discussion



Empirical atmospheric thresholds for flash events

T. Turkington et al.

Title Page

Abstract

Introduction

Conclusions

References

Tables

Figures



Back

Close

Full Screen / Esc

Printer-friendly Version

Interactive Discussion

- Intense locally driven convection appears to be the main meteorological trigger for flash events in the study area (over 66 % of events). Under these conditions, precipitation can be confined to a small area, and may explain why high precipitation values were not always recorded by the local weather stations.
- 5 – Different atmospheric indicators in spring and summer support snowmelt being an important antecedent condition for flash events in the study area in the spring.
- Even though the atmospheric thresholds performed better, there was still the high level of uncertainty in both the probabilistic thresholds and the static thresholds. This was especially true for the synoptic rainfall events. However, for the synoptic flash events, the inventory of events is one of the limiting factors and makes it difficult for further researcher using empirical thresholds.
- 10 – The methodology also needs to be trialled in other locations. It may be that in areas where there is a stronger relationship between the local weather stations and rainfall at the location of the flash events that intensity–duration thresholds are more suitable.

Acknowledgements. This work was undertaken as part of the EU FP7 Marie Curie ITN project “CHANGES” under Grant Agreement No. 263953. The authors would like to thank J.P Malet and A. Remaître for their input and help with collection of data. Data were provided by Météo France, and the ECMWF ERA-Interim data used in this study was obtained from the ECMWF data server.

References

Aleotti, P.: A warning system for rainfall-induced shallow failures, Eng. Geol., 73, 247–265, 2004. 759, 760

Alexandersson, H.: A homogeneity test applied to precipitation data, J. Climatol., 6, 661–675, doi:10.1002/joc.3370060607, 1986. 763



Empirical atmospheric thresholds for flash events

T. Turkington et al.

Title Page

Abstract

Introduction

Conclusions

References

Tables

Figures

◀

▶

◀

▶

Back

Close

Full Screen / Esc

Printer-friendly Version

Interactive Discussion



- Ansari, Z., Ahmed, W., Azeem, M. F., and Babu, A. V.: Quantitative evaluation of performance and validity indices for clustering the web navigation sessions, *World of Computer Science and Information Technology Journal*, 1, 217–226, 2011. 768
- 5 Baldi, P., Brunak, S., Chauvin, Y., Andersen, C. A. F., and Nielsen, H.: Assessing the accuracy of prediction algorithms for classification: an overview, *Bioinformatics*, 16, 412–424, 2000. 770
- Berti, M., Martina, M. L. V., Franceschini, S., Pignone, S., Simoni, A., and Pizziolo, M.: Probabilistic rainfall thresholds for landslide occurrence using a Bayesian approach, *J. Geophys. Res.-Earth*, 117, F04006, doi:10.1029/2012jf002367, 2012. 759, 761, 765, 769, 773, 775
- 10 Breinl, K., Turkington, T., and Stowasser, M.: Stochastic generation of multi-site daily precipitation for applications in risk management, *J. Hydrol.*, 498, 23–35, 2013. 790
- Brunetti, M. T., Peruccacci, S., Rossi, M., Luciani, S., Valigi, D., and Guzzetti, F.: Rainfall thresholds for the possible occurrence of landslides in Italy, *Nat. Hazards Earth Syst. Sci.*, 10, 447–458, doi:10.5194/nhess-10-447-2010, 2010. 759, 760
- 15 Brunetti, M. T., Luino, F., Vennari, C., Peruccacci, S., Biddoccu, M., Valigi, D., Luciani, S., Cirio, C. G., Rossi, M., Nigrelli, G., Ardizzone, F., Palma, M., and Guzzetti, F.: Rainfall thresholds for possible occurrence of shallow landslides and debris flows in Italy, in: *Dating Torrential Processes on Fans and Cones*, edited by: Schneuwly-Bollschweiler, M., Stoffel, M., and Rudolf-Miklau, F., Springer, Netherlands, 327–339, 2013. 758, 759, 760
- 20 Caine, N.: The rainfall intensity: duration control of shallow landslides and debris flows, *Geogr. Ann. A*, 62, 23–27, 1980. 760
- Carrara, A., Crosta, G., and Frattini, P.: Geomorphological and historical data in assessing landslide hazard, *Earth Surf. Proc. Land.*, 28, 1125–1142, doi:10.1002/esp.545, 2003. 764
- Cepeda, J., Colonnelli, S., Kronholm, K., Ferrari, A., Laloui, L., Eichenberger, J., Marvuglia, A., 25 Versace, P., Gualtieri, C. M., Remaître, A., Malet, J. P., Narasimhan, H., and Faber, M.: Statistical and empirical models for prediction of precipitation-induced landslides, Report D1.5, *SafeLand: living with landslide risk in Europe*, 137 pp., available at: http://www.safeland-fp7.eu/results/Documents/D1.5_revised.pdf, 2010. 760, 764, 774
- Chen, S.-T., Yu, P.-S., and Tang, Y.-H.: Statistical downscaling of daily precipitation using support vector machines and multivariate analysis, *J. Hydrol.*, 385, 13–22, 2010. 762, 764
- 30 Dee, D. P., Uppala, S. M., Simmons, A. J., Berrisford, P., Poli, P., Kobayashi, S., Andrae, U., Balmaseda, M. A., Balsamo, G., Bauer, P., Bechtold, P., Beljaars, A. C. M., van de Berg, L., Bidlot, J., Bormann, N., Delsol, C., Dragani, R., Fuentes, M., Geer, A. J., Haimberger, L.,

Empirical atmospheric thresholds for flash events

T. Turkington et al.

Title Page

Abstract

Introduction

Conclusions

References

Tables

Figures

◀

▶

◀

▶

Back

Close

Full Screen / Esc

Printer-friendly Version

Interactive Discussion

Healy, S. B., Hersbach, H., Hólm, E. V., Isaksen, L., Kållberg, P., Köhler, M., Matricardi, M., McNally, A. P., Monge-Sanz, B. M., Morcrette, J. J., Park, B. K., Peubey, C., de Rosnay, P., Tavolato, C., Thépaut, J. N., and Vitart, F.: The ERA-Interim reanalysis: configuration and performance of the data assimilation system, *Q. J. Roy. Meteor. Soc.*, 137, 553–597, 2011. 762, 764, 765, 778

D'Este, C., and Rahman, A.: Similarity weighted ensembles for relocating models of rare events, in: *Multiple Classifier Systems*, edited by: Zhou, Z. H., Roli, F., and Kittler, J., Springer, Berlin, Heidelberg, 25–36, 2013. 770

Done, J., Craig, G., Gray, S., Clark, P., and Gray, M.: Mesoscale simulations of organized convection: importance of convective equilibrium, *Q. J. Roy. Meteor. Soc.*, 132, 737–756, doi:10.1256/qj.04.84, 2006. 766, 767

Flageollet, J.-C., Maquaire, O., Martin, B., and Weber, D.: Landslides and climatic conditions in the Barcelonnette and Vars basins (Southern French Alps, France), *Geomorphology*, 30, 65–78, doi:10.1016/s0169-555x(99)00045-8, 1999. 763

Frattini, P., Crosta, G., and Sosio, R.: Approaches for defining thresholds and return periods for rainfall-triggered shallow landslides, *Hydrol. Process.*, 23, 1444–1460, doi:10.1002/hyp.7269, 2009. 759

Giannecchini, R.: Relationship between rainfall and shallow landslides in the southern Apuan Alps (Italy), *Nat. Hazards Earth Syst. Sci.*, 6, 357–364, doi:10.5194/nhess-6-357-2006, 2006. 759, 760

Guzzetti, F., Peruccacci, S., Rossi, M., and Stark, C.: Rainfall thresholds for the initiation of landslides in central and southern Europe, *Meteorol. Atmos. Phys.*, 98, 239–267, doi:10.1007/s00703-007-0262-7, 2007. 760

Guzzetti, F., Peruccacci, S., Rossi, M., and Stark, C.: The rainfall intensity/duration control of shallow landslides and debris flows: an update, *Landslides*, 5, 3–17, 2008. 759, 760

Huth, R., Beck, C., Philipp, A., Demuzere, M., Ustrnul, Z., Cahynová, M., Kyselý, J., and Tveito, O. E.: Classifications of atmospheric circulation patterns, *Ann. NY Acad. Sci.*, 1146, 105–152, 2008. 768

Ibsen, M. L. and Brunsden, D.: The nature, use and problems of historical archives for the temporal occurrence of landslides, with specific reference to the south coast of Britain, Ventnor, Isle of Wight, *Geomorphology*, 15, 241–258, 1996. 764

Jaiswal, P. and van Westen, C. J.: Estimating temporal probability for landslide initiation along transportation routes based on rainfall thresholds, *Geomorphology*, 112, 96–105, 2009. 773

Empirical atmospheric thresholds for flash events

T. Turkington et al.

Title Page

Abstract

Introduction

Conclusions

References

Tables

Figures

◀

▶

◀

▶

Back

Close

Full Screen / Esc

Printer-friendly Version

Interactive Discussion

- Nuissier, O., Ducrocq, V., Ricard, D., Lebeaupein, C., and Anquetin, S.: A numerical study of three catastrophic precipitating events over southern France. I: Numerical framework and synoptic ingredients, *Q. J. Roy. Meteor. Soc.*, 134, 111–130, 2008. 767
- Niall, S. and Walsh, K.: The impact of climate change on hailstorms in southeastern Australia, *Int. J. Climatol.*, 25, 1933–1952, 2005. 761
- Nuissier, O., Joly, B., Joly, A., Ducrocq, V., and Arbogast, P.: A statistical downscaling to identify the large-scale circulation patterns associated with heavy precipitation events over southern France, *Q. J. Roy. Meteor. Soc.*, 137, 1812–1827, doi:10.1002/qj.866, 2011. 775, 778
- Parajka, J., Kohnová, S., Bálint, G., Barbuc, M., Borga, M., Claps, P., Cheval, S., Dumitrescu, A., Gaume, E., Hlavčová, K., Merz, R., Pfaundler, M., Stancalie, G., Szolgay, J., and Blöschl, G.: Seasonal characteristics of flood regimes across the Alpine–Carpathian range, *J. Hydrol.*, 394, 78–89, doi:10.1016/j.jhydrol.2010.05.015, 2010. 761
- Petrow, T., Zimmer, J., and Merz, B.: Changes in the flood hazard in Germany through changing frequency and persistence of circulation patterns, *Nat. Hazards Earth Syst. Sci.*, 9, 1409–1423, doi:10.5194/nhess-9-1409-2009, 2009. 762
- Pettitt, A. N.: A non-parametric approach to the change-point problem, *J. Roy. Stat. Soc. C-App.*, 28, 126–135, 1979. 762
- Pistotnik, G., Schneider, S., and Wittmann, C.: Detection of convective initiation by objective analysis methods and its use for precipitation nowcasting, 6th European Conference on Severe Storms, 3–7 October 2011, Palma de Mallorca, Spain, 2011. 763
- Powers, D. M. W.: Evaluation: from precision, recall and F-measure to ROC, informedness, markedness & correlation, *J. Mach. Lear. Tech.*, 2, 37–67, 2011. 775
- Quan Luna, B., Blahut, J., van Westen, C. J., Sterlacchini, S., van Asch, T. W. J., and Akbas, S. O.: The application of numerical debris flow modelling for the generation of physical vulnerability curves, *Nat. Hazards Earth Syst. Sci.*, 11, 2047–2060, doi:10.5194/nhess-11-2047-2011, 2011. 770
- Rousseeuw, P.: Silhouettes: a graphical aid to the interpretation and validation of cluster analysis, *J. Comput. Appl. Math.*, 20, 53–65, 1987. 759
- Schmidli, J., Goodess, C. M., Frei, C., Haylock, M. R., Hundscha, Y., Ribalaygua, J., and Schmith, T.: Statistical and dynamical downscaling of precipitation: an evaluation and comparison of scenarios for the European Alps, *J. Geophys. Res.-Atmos.*, 112, D04105, doi:10.1029/2005jd007026, 2007. 768

Empirical atmospheric thresholds for flash events

T. Turkington et al.

Title Page

Abstract

Introduction

Conclusions

References

Tables

Figures

⏪

⏩

◀

▶

Back

Close

Full Screen / Esc

Printer-friendly Version

Interactive Discussion



- Seltzer, M. A., Passarelli, R. E., and Emanuel, K. A.: The possible role of symmetric instability in the formation of precipitation bands, *J. Atmos. Sci.*, 42, 2207–2219, 1985. 762
- Sene, K.: Debris flows, in: *Flash Floods*, Springer, Netherlands, 271–291, doi:10.1007/978-94-007-5164-4_9, 2013. 765
- 5 Tapiador, F. J., Turk, F. J., Petersen, W., Hou, A. Y., García-Ortega, E., Machado, L. A. T., Angelis, C. F., Salio, P., Kidd, C., Huffman, G. J., and de Castro, M.: Global precipitation measurement: methods, datasets and applications, *Atmos. Res.*, 104–105, 70–97, 2012. 759
- Tarolli, P., Borga, M., Morin, E., and Delrieu, G.: Analysis of flash flood regimes in the North-
10 Western and South-Eastern Mediterranean regions, *Nat. Hazards Earth Syst. Sci.*, 12, 1255–1265, doi:10.5194/nhess-12-1255-2012, 2012. 762
- Tobin, C., Nicotina, L., Parlange, M. B., Berne, A., and Rinaldo, A.: Improved interpolation of meteorological forcings for hydrologic applications in a Swiss Alpine region, *J. Hydrol.*, 401, 77–89, doi:10.1016/j.jhydrol.2011.02.010, 2011. 759, 764
- 15 Trapp, R., Diffenbaugh, N., and Gluhovsky, A.: Transient response of severe thunderstorm forcing to elevated greenhouse gas concentrations, *Geophys. Res. Lett.*, 36, L01703, doi:10.1029/2008GL036203, 2009. 760
- van Asch, T. W. J., Tang, C., Alkema, D., Zhu, J., and Zhou, W.: An integrated model to assess critical rainfall thresholds for run-out distances of debris flows, *Nat. Hazards*, 70, 299–31,
20 doi:10.1007/s11069-013-0810-z, 2014. 761, 775
- Wang, X., Chen, H., Wu, Y., Feng, Y., and Pu, Q.: New techniques for the detection and adjustment of shifts in daily precipitation data series, *J. Appl. Meteorol. Clim.*, 49, 2416–2436, doi:10.1175/2010jamc2376.1, 2010. 759
- 25 Wijngaard, J. B., Klein Tank, A. M. G., and Können, G. P.: Homogeneity of 20th century European daily temperature and precipitation series, *Int. J. Climatol.*, 23, 679–692, 2003. 763
763

Empirical atmospheric thresholds for flash events

T. Turkington et al.

Table 2. ERA-interim variables used in this study, along with abbreviations used. A brief description of each variable is also given.

Variable	Pressure level	Description
Precipitation (RR)	Surface	Rain and snow
CAPE	Surface	Estimate of instability of the atmosphere
Soil moisture (SWL)	Surface	Soil moisture for top layer (0–7 cm).
Specific humidity (Q)	850 hPa, 700 hPa, 500 hPa	Atmospheric moisture
U and V wind	10 m, 850 hPa, 700 hPa, 500 hPa	Meridional (V) and zonal (U) wind speed
Temperature (T)	850 hPa, 700 hPa, 500 hPa, 250 hPa	Temperature
Vorticity (Vo)	850 hPa, 700 hPa, 500 hPa, 250 hPa	Local spinning motion of the air
Divergence (D)	850 hPa, 700 hPa, 500 hPa	Expansion or spreading out of a vector field

Title Page

Abstract

Introduction

Conclusions

References

Tables

Figures

⏪

⏩

◀

▶

Back

Close

Full Screen / Esc

Printer-friendly Version

Interactive Discussion

Empirical atmospheric thresholds for flash events

T. Turkington et al.

Title Page

Abstract

Introduction

Conclusions

References

Tables

Figures

◀

▶

◀

▶

Back

Close

Full Screen / Esc

Printer-friendly Version

Interactive Discussion

Table 3. Classification of the flash events in the calibration period 1989–2003. The list contains the date of event, the t_{CAPE} value, and its category: Ls – local rainfall, spring Lr – local rainfall, summer, Ss synoptic rainfall, spring, Sr synoptic rainfall, summer.

Local convection				Synoptic			
Date	t_{CAPE}	Group		Date	t_{CAPE}	Group	
1.	18 Jun 1989	7	Ls	1.	3 Nov 1991	–1	Sr
2.	14 Aug 1990	13	Lr	2.	2 Jun 1992	–1	Ss
3.	29 Sep 1991	46	Lr	3.	12 Jul 1993	0	Sr
4.	6 Oct 1991	24	Lr	4.	11 May 1994	0	Ss
5.	1 Jun 1992	19	Ls	5.	13 May 1994	0	Ss
6.	18 Jun 1992	93	Ls	6.	6 Jul 1996	0	Sr
7.	21 Jul 1992	8	Lr	7.	19 Aug 1996	1	Sr
8.	27 Sep 1992	9	Ls	8.	25 Jul 1997	0	Sr
9.	10 Jul 1993	12	Ls	9.	22 Mar 2001	0	Ss
10.	5 Nov 1994	77	Lr				
11.	28 Aug 1997	9	Lr				
12.	12 Aug 2000	9	Lr				
13.	13 Aug 2000	20	Lr				
14.	23 Nov 2000	8	Lr				
15.	26 Jul 2001	55	Lr				
16.	5 Jun 2002	27	Ls				
17.	23 Jun 2002	15	Ls				
18.	27 Jul 2003	10	Lr				
19.	5 Aug 2003	110	Lr				
20.	8 Aug 2003	20	Lr				

Empirical atmospheric thresholds for flash events

T. Turkington et al.

Title Page

Abstract

Introduction

Conclusions

References

Tables

Figures

⏪

⏩

◀

▶

Back

Close

Full Screen / Esc

Printer-friendly Version

Interactive Discussion

Table 4. Results for the static threshold for the calibration period (1989–2003) and validation period 1 (1979–1988) and validation period 2 (2004–2010). The total number of days (TP + FN + FP + TN) is the same for the weather station and local convection. The number is lower for Ss and Sr, as they are only applied over spring and summer respectively.

	TP	FN	FP	TN	MCC
Weather station					
Calibration	16	13	412	5037	0.13
Validation 1	10	18	244	3381	0.10
Validation 2	2	4	145	2406	0.06
Local convection					
Calibration	15	5	332	5126	0.17
Validation 1	14	5	255	3397	0.18
Validation 2	4	1	171	2381	0.13
Synoptic – snowmelt					
Calibration	2	2	93	2198	0.10
Validation 1	1	2	105	1422	0.05
Validation 2	0	0	70	967	–
Synoptic – rainfall					
Calibration	3	2	193	2097	0.09
Validation 1	0	6	115	1409	0
Validation 2	0	1	60	1010	0

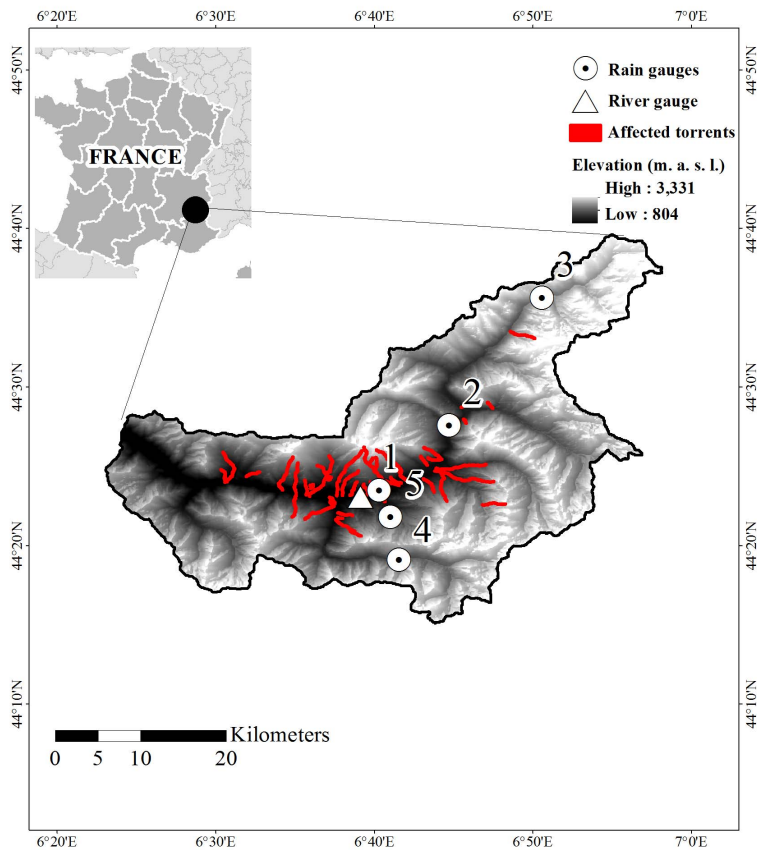


Fig. 1. The study area including the location of rain gauges and a single river gauging station. Red lines depicts the affected torrents where debris flows or flash floods occurred between 1979 and 2010 (map based on Breinl et al., 2013).

Empirical atmospheric thresholds for flash events

T. Turkington et al.

Title Page

Abstract Introduction

Conclusions References

Tables Figures

⏪ ⏩

◀ ▶

Back Close

Full Screen / Esc

Printer-friendly Version

Interactive Discussion



Empirical atmospheric thresholds for flash flood events

T. Turkington et al.

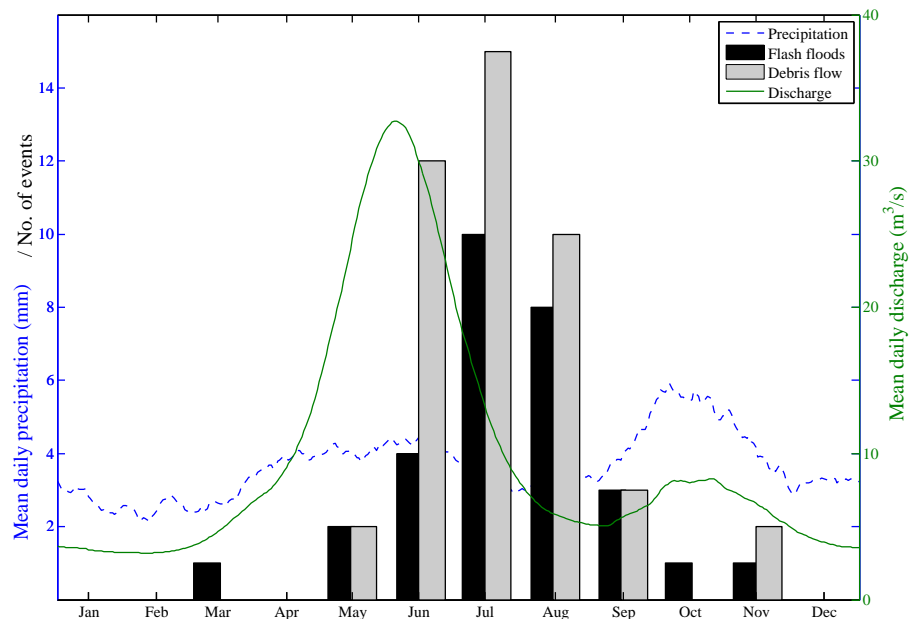


Fig. 2. Running 30 day mean daily precipitation and discharge for the period 1979–2009, for the Barcelonnette weather station and river gauge in the Ubaye River. The bar graph displays the number of flash floods and debris flows observed between 1979 and 2010.

Empirical atmospheric thresholds for flash events

T. Turkington et al.

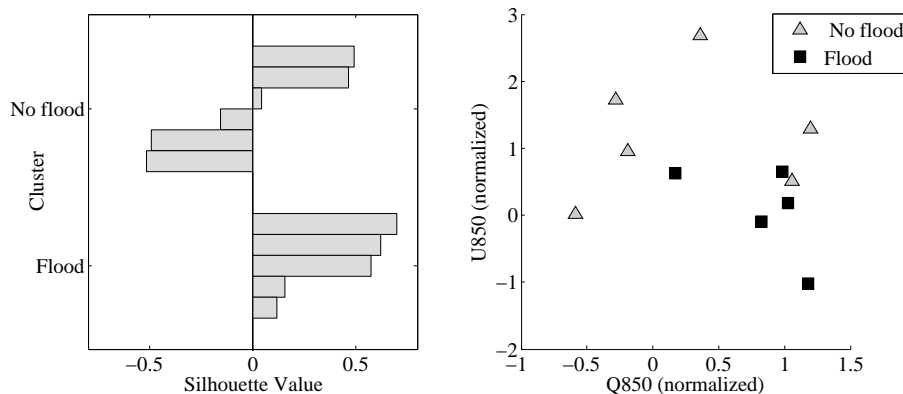


Fig. 3. A worked example of calculating SI values. The right side plots the specific humidity at 850 hPa and U wind at 850 hPa for five flood days and six non-flood days. These values were then used to derive the individual silhouette values in the plot on the left.

Title Page

Abstract

Introduction

Conclusions

References

Tables

Figures

◀

▶

◀

▶

Back

Close

Full Screen / Esc

Printer-friendly Version

Interactive Discussion

Empirical atmospheric thresholds for flash events

T. Turkington et al.

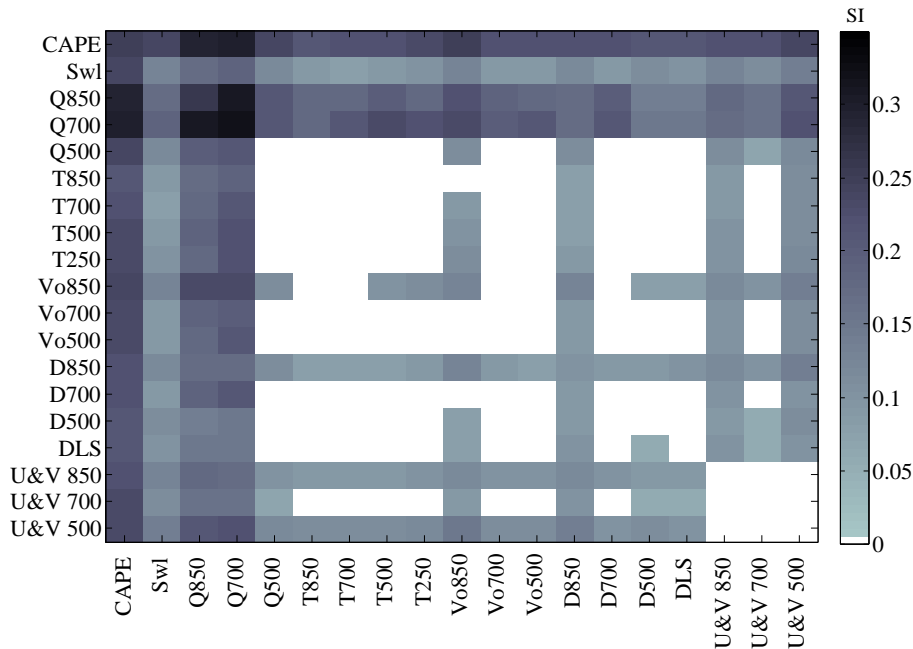


Fig. 4. The SI value for each pair of atmospheric indicators in Table 2 for local convection events using daily values. Any value that was not significant at $p = 0.05$ level was given a value of zero.

Title Page

Abstract Introduction

Conclusions References

Tables Figures

⏪ ⏩

◀ ▶

Back Close

Full Screen / Esc

Printer-friendly Version

Interactive Discussion



Empirical atmospheric thresholds for flash events

T. Turkington et al.

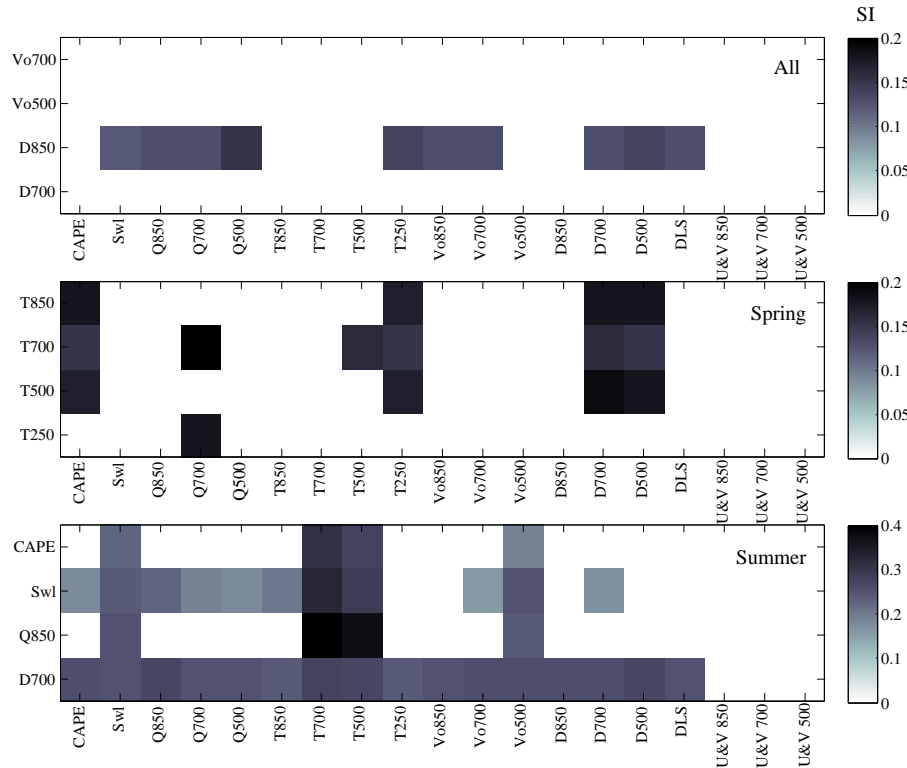


Fig. 5. Top: the SI value for each pair of atmospheric indicators for all synoptic events using the daily value and the mean value over 10 days. Middle: the SI value for each pair of atmospheric indicators for the Ss events (3 day and 8 day averages). Bottom: the SI value for each pair of atmospheric indicators for Sr using (daily value and 8 day average). Any value that was not significant at $p = 0.10$ level was given a value of zero.

Title Page

Abstract Introduction

Conclusions References

Tables Figures

◀ ▶

◀ ▶

Back Close

Full Screen / Esc

Printer-friendly Version

Interactive Discussion



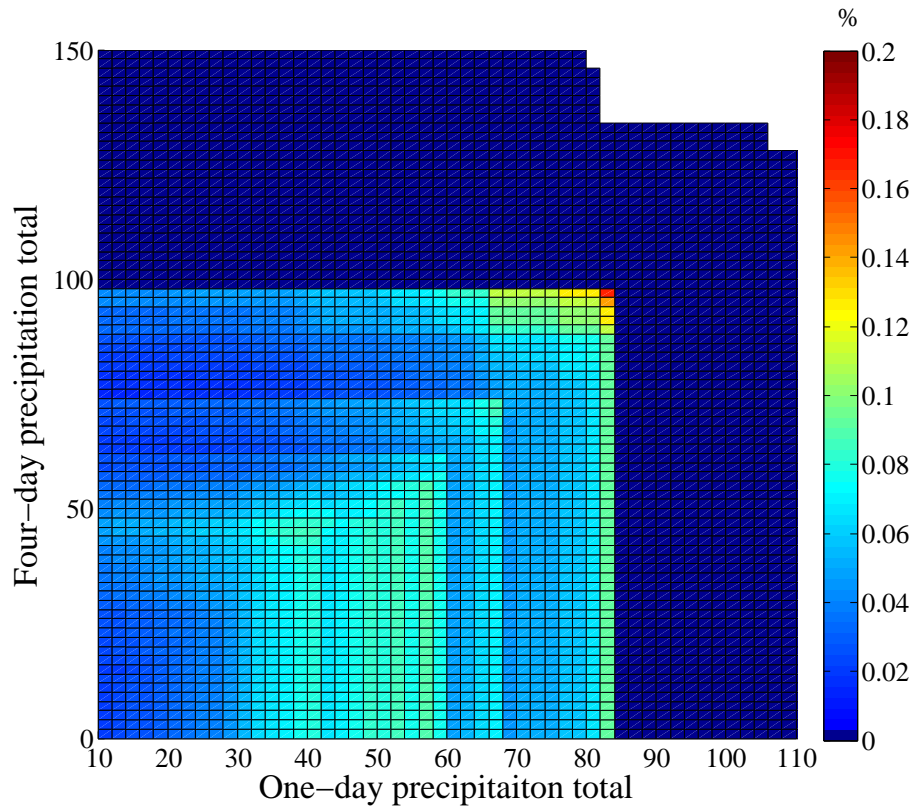


Fig. 6. Probability of a flash event based on 1 day and 4 day precipitation totals from a local rain gauge. Dark blue indicates zero probability of occurrence.

Empirical atmospheric thresholds for flash events

T. Turkington et al.

Title Page	
Abstract	Introduction
Conclusions	References
Tables	Figures
◀	▶
◀	▶
Back	Close
Full Screen / Esc	
Printer-friendly Version	
Interactive Discussion	



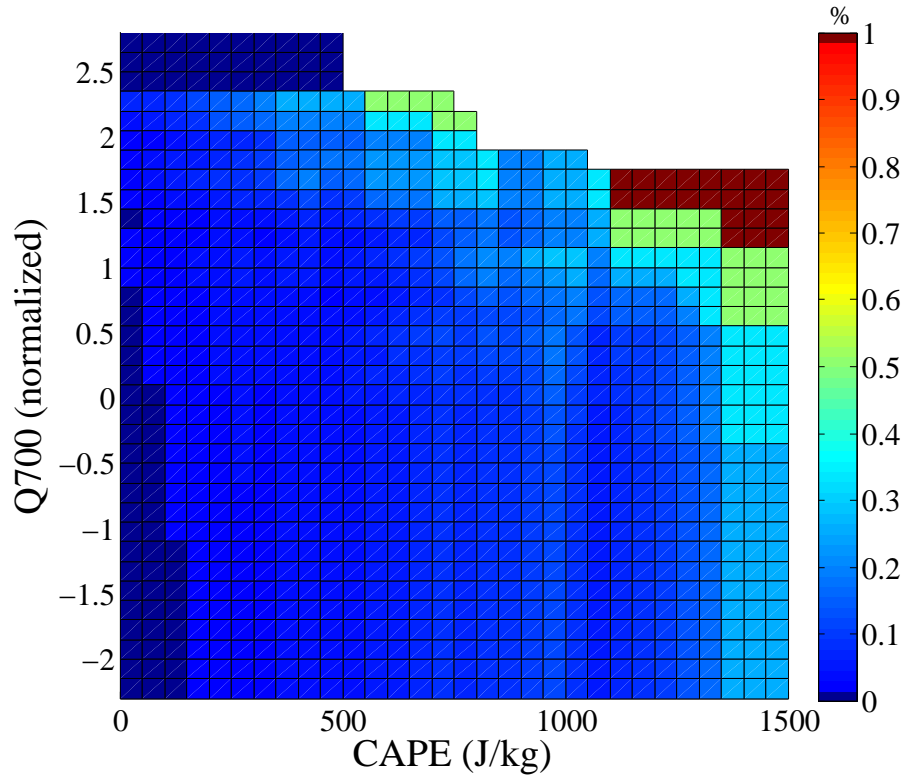


Fig. 7. Probability of a local convection flash event based on atmospheric indicators CAPE and normalized specific humidity at 700 hPa (between 1989–2003).

**Empirical
atmospheric
thresholds for flash
events**

T. Turkington et al.

Title Page

Abstract Introduction

Conclusions References

Tables Figures

⏪ ⏩

◀ ▶

Back Close

Full Screen / Esc

Printer-friendly Version

Interactive Discussion



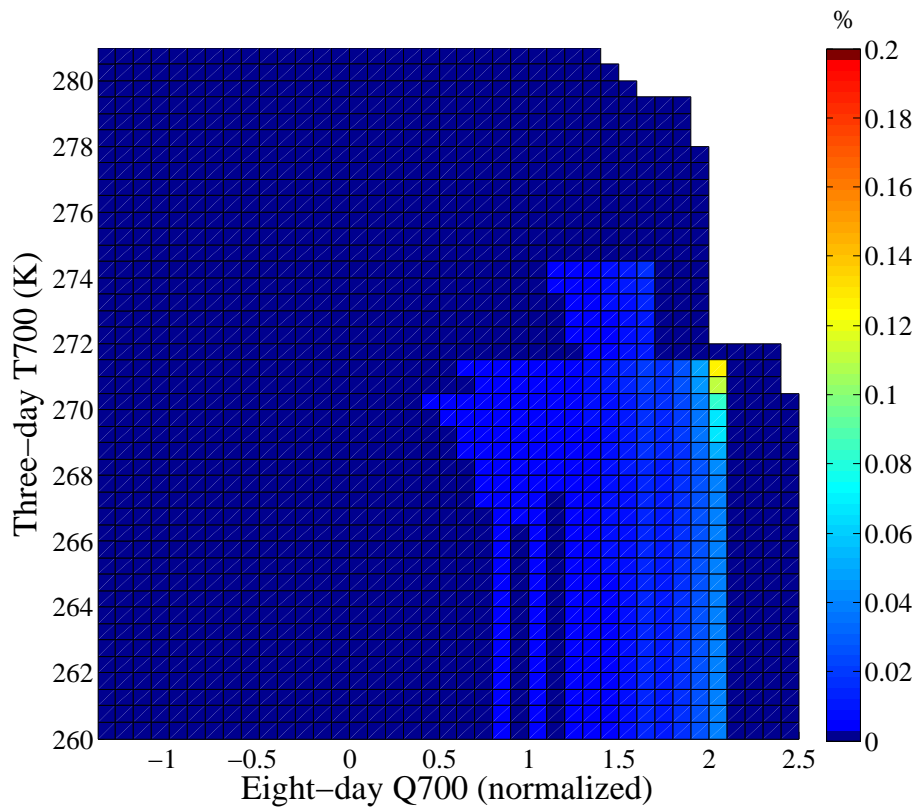


Fig. 8. Probability of a flash event from spring synoptic rainfall based on eight-day mean specific humidity at 700 hPa and three-day mean temperature at 700 hPa between 1989–2003.

**Empirical
atmospheric
thresholds for flash
events**

T. Turkington et al.

Title Page

Abstract Introduction

Conclusions References

Tables Figures

◀ ▶

◀ ▶

Back Close

Full Screen / Esc

Printer-friendly Version

Interactive Discussion



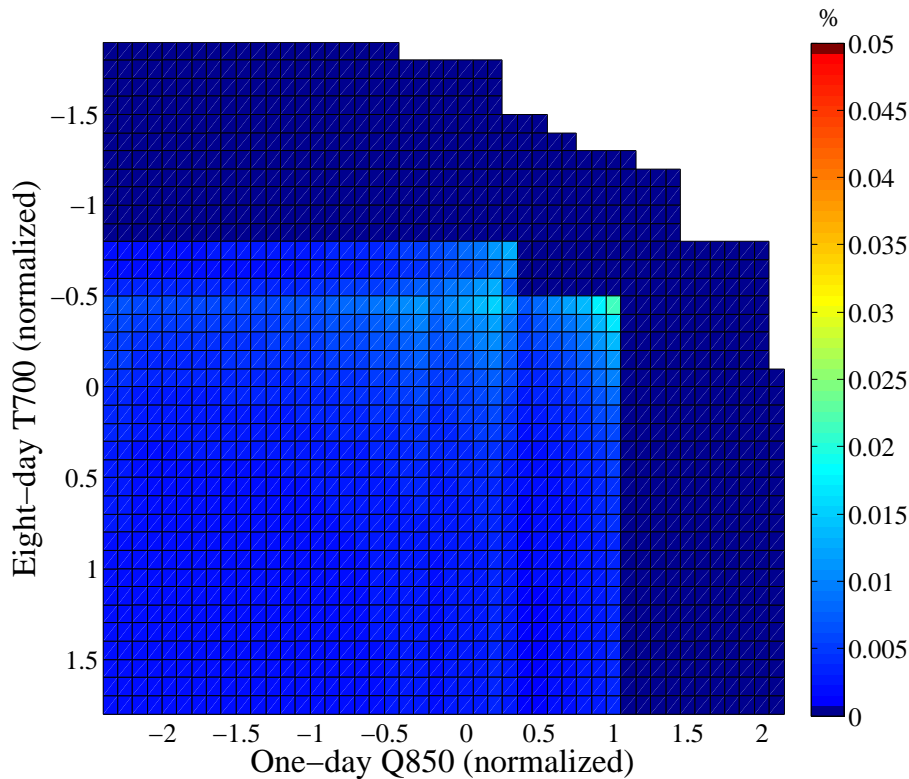


Fig. 9. Probability of a flash event from summer synoptic rainfall based on eight-day mean temperature at 700 hPa and three-day mean specific humidity at 850 hPa between 1989–2003. The y-axis is inverted to highlight that the figure represents the probability of a flash event given that $T700$ is less than the a particular value and $Q850$ is greater than a particular value.

Empirical atmospheric thresholds for flash events

T. Turkington et al.

Title Page

Abstract

Introduction

Conclusions

References

Tables

Figures

◀

▶

◀

▶

Back

Close

Full Screen / Esc

Printer-friendly Version

Interactive Discussion

